Spectroscopic Comparisons of the pH Dependencies of Fe-Substituted (Mn)Superoxide Dismutase and Fe-Superoxide Dismutase[†]

Carrie K. Vance and Anne-Frances Miller*

Jenkins Department of Biophysics and Department of Chemistry, The Johns Hopkins University, 3400 North Charles Street, Baltimore, Maryland 21218

ABSTRACT: We have compared the active sites of *Escherichia coli* Fe-substituted (Mn)superoxide dismutase [Fe-sub-(Mn)SOD] and Fe-SOD to elucidate the basis for the inactivity of Fe-sub-(Mn)SOD, despite its apparent similarity to Fe-SOD. The active site of (reduced) Fe^{2+}-sub-(Mn)SOD is qualitatively similar to that of native Fe^{2+}-SOD, indicating similar active site structures and coordination environments for Fe^{2+}. Its nativelike pK is indicative of nativelike local electrostatics, and consistent with Fe^{2+}-sub-(Mn)-SOD's retention of ability to reduce $O_2^{\bullet-}$ [Vance and Miller (1998) *J. Am. Chem. Soc. 120*(3), 461−467]. The active site of (oxidized) Fe^{3+}-sub-(Mn)SOD differs from that of Fe^{3+}-SOD with respect to the EPR signals produced at both neutral and high pH, indicating different coordination environments for Fe^{3+}. Although Fe^{3+}-sub-(Mn)SOD binds the small anions N_3^- and F^-, the K_D for N_3^- is tighter than that of Fe^{3+}-SOD, suggesting that the (Mn)SOD protein favors anion binding more than does the (Fe)SOD protein. The EPR spectral consequences of binding F^- are reminiscent of those observed upon binding the first F^- to Fe^{3+}-SOD, but the EPR spectrum obtained upon binding N_3^- is different, consistent with crystallographic observation of a different binding mode for N_3^- in *Thermus thermophilus* Mn-SOD than Fe-SOD [Lah, M., et al. (1995) *Biochemistry 34*, 1646−1660]. We find a pK of 8.5 to be associated with dramatic changes in the EPR spectrum. In addition, we confirm the pK between 6 and 7 that has previously been reported based on changes in the optical signal and N_3^- binding [Yamakura, F., et al. (1995) *Eur. J. Biochem. 227*, 700−706]. However, this latter pK appears to be associated with much subtler changes in the EPR spectrum. The non-native pKs observed in Fe^{3+}-sub-(Mn)SOD and the differences in the Fe^{3+} coordination indicated by the EPR spectra are consistent with Fe^{3+}-sub-(Mn)SOD's inability to oxidize $O_2^{\bullet-}$ and suggest that its low $E°$ is due to perturbation of the oxidized state.

In enzymes with a catalytically active metal ion, the identity of the metal determines what chemistry is possible, but the protein specifies and controls the chemistry that actually occurs.

The first coordination shell comprises the ligands, whose identities, number, disposition and ionization states define the geometry of the metal ion, determine whether and which substrates can coordinate directly, and set the reduction midpoint potential ($E°$), which is a fundamental determinant of activity (reviewed in ref. *1*). The second shell influences the activity of the metal ion by determining the polarity of the environment and modulating the properties of the ligands. Hydrogen bonds and electrostatic interactions that modify the distribution of ligand electron density have large influences on the ligand pKs and the metal ion $E°$ (*2, 3*). Second shell residues also aid in substrate binding, and can even participate in catalysis by donating or accepting protons. Thus, the protonation states of ligands and second sphere residues are crucial to the nature of these residues' interactions with each other and their influence on the activity of the metal ion.

Despite their importance in determining the metal center activity, the effects of second sphere interactions are subtler than those of ligands, and not nearly as well understood. This is partly because the collective and indirect nature of second sphere effects makes them more difficult to address by model studies. The Fe- and Mn-specific superoxide dismutases (SODs)[1] are an ideal system in which to address the significance of the protein around the ligand sphere because the two SODs employ the same amino acid ligands
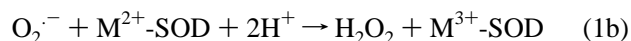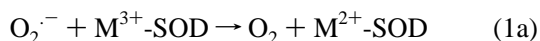
[1] Abbreviations: Asp, aspartate; Arg, arginine; DPPH, α,α′-diphenyl-β-picrylhydrazine; DSS, 4,4-dimethyl-4-silapentane sulfonate sodium salt; EPR, electron paramagnetic resonance spectroscopy; EXAFS, extended X-ray absorbance fine structure spectroscopy; Fe-SOD, Fe-containing superoxide dismutase; (Fe)SOD, protein of Fe-SOD; Fe-sub-(Mn)SOD, Fe-substituted into (Mn)SOD protein; Gln, glutamine; His, histidine; ICP-OES, inductively coupled plasma optical emission spectroscopy; LMCT, ligand to metal charge transfer; Mn-SOD, Mn-containing superoxide dismutase; (Mn)SOD, protein of Mn-SOD; Mn-sub-(Fe)SOD, Mn-substituted into (Fe)SOD protein; NAS, non active site; NBT, nitroblue tetrazolium; NHE, normal hydrogen electrode; NMR, nuclear magnetic resonance spectroscopy; Phe, phenylalanine; SDS−PAGE, sodium dodecyl sulfate−polyacrylamide gel electrophoresis; SOD, superoxide dismutase; Tyr, tyrosine; WEFT, water-eliminated Fourier transform; Y34F, Tyr 34 to Phe mutant.

and the same overall structure and both bind either metal ion. However, differences in their second spheres are held responsible for the fact that each is active under standard conditions only with its native metal ion bound.

SOD catalyzes the disproportionation of $O_2^{\bullet-}$ to O_2 and H_2O_2 by a two-step reaction in which the Fe or Mn ion alternates between the $+3$ and $+2$ oxidation states (*4*).

$$O_2^{\cdot-} + M^{3+}\text{-SOD} \rightarrow O_2 + M^{2+}\text{-SOD} \qquad (1a)$$

$$O_2^{\cdot-} + M^{2+}\text{-SOD} + 2H^+ \rightarrow H_2O_2 + M^{3+}\text{-SOD} \qquad (1b)$$

where M signifies the bound metal ion. Although Fe- and Mn-specific SODs are very closely related to one another, they are essentially unrelated to the Cu and Zn-containing SODs.

Fe- and Mn-SODs are dimers or tetramers of identical monomers, which each have one active site containing a single Fe or Mn ion. The overall folds are the same, and in both cases the metal ion is coordinated in a trigonal bipyramid by two His and an Asp^- in the equatorial plane and a His and a solvent molecule as axial ligands (*5*). The coordinated solvent is believed to be H_2O in (reduced) Fe^{2+}-SOD and to donate a proton to substrate upon oxidation of Fe to become OH^- in (oxidized) Fe^{3+}-SOD (*6*).

The amino acids immediately surrounding the active site are especially highly conserved among Fe- and Mn-SODs. In particular, His 30 and Tyr 34,[2] which may donate the other of the two protons transferred to substrate (*7*), are universally conserved. A hydrophobic shell surrounding the active site is also strongly conserved. However, there are a few conserved differences. Most notably, the active site Gln is derived from position 141 in Mn-SODs but position 69 in Fe-SODs. The side chain of this Gln is believed to hydrogen bond with both Tyr 34 and the coordinated solvent.

More than 20 years after the initial observation (*8*), we are finally beginning to understand why Mn-SOD protein with Fe bound instead of Mn [Fe-sub-(Mn)SOD][3] appears inactive, as does Mn-sub-(Fe)SOD. Yamakura and colleagues have shown that Fe-sub-(Mn)SOD from both *Serratia marcescens* and *Escherichia coli* display increased activity at low pH (*9, 10*). Increases in activity and anion binding, and changes in the optical and the EPR signal, all correlate with a pK of ≈ 7 in *S. marcescens* Fe^{3+}-sub-(Mn)-SOD (*10*), and changes in the optical signal and increased activity are associated with a pK of ≈ 6 in Fe^{3+}-sub-(Mn)-SOD from *E. coli* (*9*). These pKs are believed to be analogous to the pK near 9 affecting Fe^{3+}-SOD (*11, 12*). Since the pK near 9 in *E. coli* Fe^{3+}-SOD is ascribed to coordination of a second OH^- to Fe^{3+} (*13, 14*), the inactivity of Fe^{3+}-sub-(Mn)SOD might be related to OH^- binding with higher-than native affinity, but with similar effects on the active site.

pH titrations of the activity and optical signal of Fe-sub-(Mn)SOD indicate that upon mutagenesis of Tyr 34 to Phe,

the pK is shifted from 6.4 to 7.9, and that this amino acid substitution also results in a substantial increase in the activity of Fe-sub-(Mn)SOD, at all pHs (*15*). Finally, Fe-sub-(Mn)-SOD has been shown to retain the ability to reduce $O_2^{\bullet-}$ but to be unable to oxidize it (*16*). This can explain Fe-sub-(Mn)SOD's apparent overall inactivity and could be due to too low an E°, or inability to correctly bind substrate. Indeed, the E° was found to be ≈ 450 mV lower than native Fe-SOD's, and is sufficiently low to explain Fe-sub's inactivity (*16*).

Thus, the apparent inactivities of Fe-sub-(Mn)SOD and Mn-sub-(Fe)SOD may reflect a mismatch between the E° of the metal ion and the E° tuning applied by the protein, which has evolved to use the native metal ion (*16, 17*). Because the E°s of the $3+/2+$ couple of high-spin Mn compounds are typically higher than the E°s of analogous high-spin Fe complexes (*18*), Mn-specific SOD proteins probably depress the E° of Mn^{3+}/Mn^{2+} more than Fe-specific SOD proteins depress that of Fe^{3+}/Fe^{2+}, to approach the $E^{\circ\prime}$ of ≈ 0.36 V (vs NHE) predicted to be optimal for SOD activity (*19*). Therefore, we have proposed that when Fe is bound in the (Mn)SOD protein, its $E^{\circ\prime}$ is depressed to a value well below the native $E^{\circ\prime}$ of $0.2-0.4$ V (*19*), and similarly that the $E^{\circ\prime}$ of Mn bound in (Fe)SOD is insufficiently depressed, to a value well above $0.2-0.4$ V (*16, 17*). This model is consistent with the increase in activity observed at low pH as protonation of the active site of Fe-sub-(Mn)-SOD would tend to raise its E° and restore its ability to oxidize $O_2^{\bullet-}$.

Fe-sub-(Mn)SOD's low E° can explain the former's inactivity, but demands an explanation itself. Furthermore, although it is sufficient to explain inactivity (*16*), other possible reasons have not been ruled out. Therefore, we have now compared Fe-SOD with Fe-sub-(Mn)SOD, with respect to active site integrity and substrate analogue binding, as well as the pKs of active site residues that interact with Fe electrostatically or via hydrogen bonds, or are ligands to Fe, since these will be important determinants of Fe's E°.

MATERIALS AND METHODS

General. Mn-SOD was overexpressed from the sodA$^-$, sodB$^-$ *E. coli* strain QC774 transformed with the sodA gene on plasmid pDT1-5 (*20*) and purified as described previously (*21*). Specific activity was determined using the standard xanthine oxidase/cytochrome *c* assay at pH 7.8 (*22*) or assayed qualitatively by resolving SOD on nondenaturing PAGE and staining with nitroblue tetrazolium (NBT) and riboflavin (*23*). Protein concentrations were determined using $\epsilon_{280} = 8660$, 9190, and 8950 M^{-1} cm^{-1} for Mn-SOD, Fe-sub-(Mn)SOD, and apo-(Mn)SOD, respectively (*24*).

Metal Ion Replacements. Apo-(Mn)SOD was prepared by dialyzing Mn-SOD into 3.5 M guanidine hydrochloride (GuHCl), 20 mM Tris-HCl, and 10 mM EDTA at pH 3.1, followed by 2.5 M GuHCl, 20 mM Tris-HCl, and 10 mM EDTA at pH 8.0, and finally 25 mM K_2HPO_4, pH 7.8, for 8 h each at 4 °C.

Fe was introduced into the (Mn)SOD active site before the protein was refolded, in contrast with earlier protocols in which apo-protein was refolded prior to a second denaturation step in which the Fe was added (*10, 25*). Thus, the third dialysis was against 2.5 M GuHCl, 20 mM Tris-HCl pH 8.0, to remove excess EDTA. The solution was

---

[2] For simplicity, the numbering of Fe-SOD from *E. coli* is used throughout, even when referring to Mn-SOD.

[3] (Mn)SOD and (Fe)SOD refer to the protein components of Mn-SOD and Fe-SOD, respectively, and Fe-sub-(Mn)SOD and Mn-sub-(Fe)SOD refer to Fe bound in (Mn)SOD protein and Mn bound in (Fe)SOD protein, respectively.

then sparged with N_2 gas for 1 h before an anaerobic solution of $FeCl_2$ was injected directly into the dialysis bag, which was resealed by clipping off the punctured area. The dialysis bag was transferred to 25 mM Tris-HCl, pH 8.0, buffer which had been sparged with N_2 for at least 15 min, and the protein was allowed to refold for 8−12 h, during which time the GuHCl dialyzed out and the solution was kept anaerobic by sparging continuously with N_2. The final Fe^{2+} concentration in the dialysis bag was 1 mM, and the (Mn)SOD concentration was 100−200 μM. To rinse the protein free of extraneous Fe before the latter could oxidize and adhere nonspecifically, the protein was dialyzed against N_2-sparged 1 mM EDTA, 25 mM Tris-HCl, pH 8.0, followed by 25 mM Tris-HCl, pH 7.8, and finally 100 mM KBr, 100 mM K_2HPO_4 at pH 7.8.

Mn-reconstituted (Mn)SOD [Mn-rec-(Mn)SOD] was produced in a similar manner as the Fe-sub-(Mn)SOD, except that $MnCl_2$ was added to the dialysis bag instead of $FeCl_2$. Protein yields were calculated from the concentrations and volumes of each sample and taken as a percentage of the starting amount of Mn-SOD.

Quantitative analysis of the ratio of Fe to protein was performed colorimetrically using the ferrozine assay with ϵ_{562} = 28 000 M^{-1} cm^{-1}, calibrated against a commercial Fe standard, and verified by ICP-MS (Galbraith Labs). EPR was also used to assess the amount of non active site (NAS) Fe in oxidized samples, based on the amplitude of the signature of rhombic Fe at $g' = 4.3$ (see Results). NAS Fe^{3+} was preferentially removed by dialyzing Fe-sub-(Mn)SOD repeatedly against anaerobic 1 mM EDTA, 1 mM ascorbate, and 20 mM Tris-HCl buffer at pH 7.8, followed by two dialyses against 100 mM KBr, 100 mM K_2HPO_4, pH 7.8.

Optical pH and Azide Titrations. Visible absorption spectra were collected on a Hewlett-Packard 8452A diode array spectrophotometer equipped with a thermostated cell compartment. pH, N_3^-, and F^- titrations were carried out in a sealed 3 mL quartz cuvette equilibrated at 25 °C. The pH was measured using a combination pH microelectrode fitted into a 12 gauge stainless-steel needle (Microelectrodes Inc.). Three milliliters of 0.1 mM Fe-sub-(Mn)SOD protein dimers was dialyzed against 100 mM KBr, 100 mM KH_2PO_4, pH 5.2, and filtered to remove precipitate before beginning the titration. The pH was increased by adding small aliquots of 100 mM KOH, using a precision Hamilton syringe. Return points were obtained similarly by adding 100 mM H_3PO_4. Addition of Cl^- ion was avoided since Cl^- binds to and inhibits Fe^{3+}-SOD (*12*). The absorbance's dependence on pH was fit using the Henderson−Hasselbalch equation.

N_3^- binding was monitored optically at various pHs by titrating 0.1 mM Fe-sub-(Mn)SOD in a sealed 1 mL quartz cuvette at 25 °C. Each sample was titrated with 1−5 μL aliquots of 1, 10, or 100 mM NaN_3, and the development of a strong shoulder at 390 nm was monitored. The pH was recorded before and after the azide additions. The apparent K_D (K_D') was determined by fitting the data at each pH with the azide-binding analogue of the Henderson−Hasselbalch equation, and the pH dependence of K_D' (corrected for the pK of N_3^-) was modeled using $K_D' = K_D[1+ 10^{(pH-pK)}]$.

EPR Spectroscopy. EPR spectra were collected on a Bruker 300MX calibrated at $g' = 2$ using DPPH and at $g' = 6$ using myoglobin in 100 mM K_2HPO_4. EPR spectra were

collected at 9.30 GHz (or 9.47 GHz) at 77 K (or 65 K), depending on whether a dewar insert (or a flow cryostat) was used, with 80 mW nominal microwave power, 2 G modulation amplitude, and 3000 G wide scans centered at 2100 G obtained in approximately 20 min. EPR signals of Fe-sub-(Mn)SOD at a range of pHs were collected at 65 K at 9.47 MHz. Five milliliters of 0.1 mM Fe^{3+}-sub-(Mn)SOD was dialyzed into 100 mM KH_2PO_4, 100 mM KBr at pH 7.0 and then filtered. The pH was raised using 5 μL aliquots of 100 mM KOH or lowered by careful additions of 100 mM H_3PO_4; 250 μL aliquots were removed to 4 mm EPR tubes, the pHs of the samples were measured, and the samples were frozen in liquid N_2. The sample pHs were measured again after collection of EPR spectra.

EPR was used to quantify the Mn content of Mn-SOD, apo-(Mn)SOD, and Fe-sub-(Mn)SOD, after incubation in 1 M HCl to release all the Mn as $Mn^{2+}(H_2O)_6$ and then addition of glycerol to 50% v/v. To detect single-digit micromolar concentrations of Mn^{2+}, signals were recorded at 77 K. The standard curve of the peak-to-trough height of the low-field peak vs Mn^{2+} concentration was linear with $R = 0.9998$, from 1 to 500 μM Mn^{2+}. This was used to determine the Mn^{2+} concentration in replicate samples of acid-denatured SOD. The percent Mn^{2+} was determined by taking the ratio of the Mn^{2+} concentration to the concentration of active sites, as determined from the ϵ_{280}. Doubly deionized H_2O from a Millipore filtering system was used exclusively.

NMR Spectroscopy. NMR spectra were collected at 30 °C on an AMX at 300 MHz for ^1H. A super-WEFT sequence with selective saturation of water was used to detect the protein active site resonances (*21, 26*). The pH was determined from the chemical shifts of internal pH indicator molecules (*21*) which were observed with a spin−echo sequence incorporating 30 ms delays to suppress protein resonances.

For each NMR sample, 450 μL of 1 mM Fe-sub-(Mn)-SOD in 100 mM K_2HPO_4 and 50 μL of ^2H_2O was degassed and reduced with 5 μL of 150 mM sodium dithionite in an NMR tube fitted with a Teflon seal. The chemical shift standard DSS and the NMR pH indicators imidazole, 2,4-dimethylimidazole, and trimethylamine were included at concentrations of 0.1, 2.0, 1.0, and 0.3 mM, respectively. The pH of the sample was adjusted using 100 mM KOH, and measured after each adjustment. The chemical shifts of the active site Fe^{2+}-sub-(Mn)SOD resonances were then plotted as functions of the pH and fit with a Henderson−Hasselbalch equation with allowance for cooperativity:

$$\frac{\delta_A - \delta_{obs}}{\delta_A - \delta_B} = \frac{K^n}{K^n + 10^{-n(pH)}}$$

where δ_A and δ_B are the chemical shifts of the acid and base forms (obtained from the fit), δ_{obs} is the observed chemical shift at a given pH, K is the acid dissociation constant obtained from the fit, and n is the Hill coefficient obtained from the fit (*27*).

RESULTS

Biochemical Characterization of Fe-sub-(Mn)SOD. Table 1 presents the results of metal ion removal and incorporation in (Mn)SOD protein from *E. coli*. The loss of activity upon

Table 1: Fe Contents, Mn Contents, and Activities of Native and Fe-Substituted SODs

sample	Fe content[a]	Mn content[b]	activity[c]
Mn-SOD	0	0.98	6800
apo-(Mn)SOD	0	0	0
Fe-SOD	0.98		6500
Fe-sub-(Mn)SOD	0.95	0	0

[a] Fe content was measured colorimetrically (36), and is expressed on a per subunit basis. The uncertainty is estimated to be 0.03 per subunit. [b] Mn content was measured by EPR, and is expressed on a per subunit basis. The detection limit is less than 1 μM Mn or 0.005 per subunit, and the uncertainty is approximately 3%. [c] Catalytic activity was measured in the standard xanthine oxidase/cytochrome c indirect assay at pH 7.8 (22) which has a detection limit corresponding to less than 0.1% of native SOD activity and an uncertainty of $\approx$100 units/mg of protein for activities in the range of 5000 units/mg.

Mn removal was measured by assaying an aliquot of (Mn)-SOD after the second dialysis in GuHCl but before Fe addition or by producing refolded apo-(Mn)SOD in parallel with the Fe-sub-(Mn)SOD. The Fe-sub-(Mn)SOD obtained typically had over 95% Fe incorporation as determined by the ferrozine colorimetric assay for Fe. In all cases, no activity could be detected by the standard xanthine oxidase/cytochrome c assay at pH 7.8 (22) for either apo-(Mn)SOD or Fe-sub-(Mn)SOD. Despite other reports (28), protein loss due to precipitation was negligible.

Our procedure does not appear to damage the (Mn)SOD protein, as Mn-rec-(Mn)SOD produced from either apo-(Mn)SOD or Fe-sub-(Mn)SOD had equal if not higher activity than the starting Mn-SOD. One sample was exposed to three metal removal and substitution cycles, successively incorporating Fe, Fe and then Mn, with recovery of over 91% of the activity of the starting material. In addition, nondenaturing PAGE results in a single band, unless sub-stoichiometric Fe is bound. Therefore, Fe-sub-(Mn)SOD's loss of activity must be ascribed to the identity of the metal ion itself and its interactions with the protein.

Competition experiments indicate that Fe binds in the active site, as reconstitution with a mixture of equal concentrations of Fe and Mn resulted in SOD with 40% of starting activity and fractional incorporation of Fe. Non-denaturing PAGE of this material revealed multiple bands, instead of the single bands obtained for each of Mn-rec- or Fe-sub-(Mn)SOD.

Specificity of Fe Binding. The primary obstacle to clean and complete metal substitution in (Mn)SOD is not difficulty achieving stoichiometric incorporation of Fe, but rather the near impossibility of avoiding nonspecific Fe binding. Unfortunately, non active site (NAS) Fe^{3+} not only exhibits strong optical absorbance, which overlaps that of active site Fe^{3+}, but also binds many of the same anions. Therefore, we used EPR spectroscopy of oxidized samples to assess the amount of NAS Fe^{3+} present, based on its distinctive rhombic signal at $g' = 4.3$ (1550 G). NAS Fe was removed by reducing the external Fe^{3+} with ascorbate and chelating with EDTA, as described under Materials and Methods. Chelation alone did not completely remove NAS Fe. Figure 1 compares the EPR signals obtained from samples after successive dialyses against EDTA and ascorbate plus EDTA at pH 7.6. Clearly, the rhombic signal at $g' = 4.3$ is largely eliminated while the active site signal is largely retained (e.g.
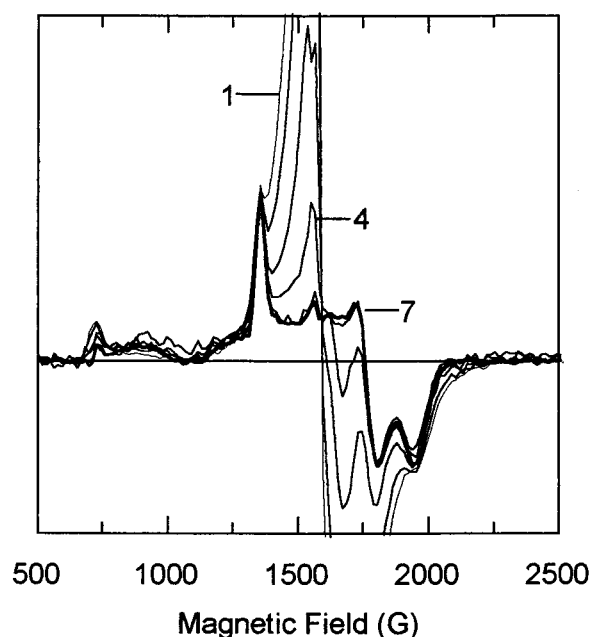

FIGURE 1: EPR spectra of Fe^{3+}-sub-(Mn)SOD after each of a series of dialyses against EDTA and ascorbate, showing the decrease in NAS Fe content. The spectra with the largest amplitude in the region of 1500−1800 G are those containing the most NAS Fe^{3+}. NAS Fe^{3+} decreased from the amount in spectrum (1) with each dialysis against (2) 1 mM EDTA, (3) 1 mM each EDTA and ascorbate, (4) 1 mM EDTA, and (5−7) 1 mM each EDTA and ascorbate. Spectra are scaled to the same active site Fe^{3+} concentration, and selected spectra are numbered in order of increasing number of NAS removal steps. Although removal of NAS Fe was typically achieved with loss of some $\approx$10% of active site Fe, active sites lacking Fe are spectroscopically silent, and the Fe-containing active sites of dimers in which the other active site lacks Fe appear to behave very similarly to the active sites in fully metalated dimers, since the activities of Fe-SOD and Mn-SOD are directly proportional to Fe and Mn content, respectively (25, 35). Conditions for NAS Fe removal and EPR spectroscopy are described under Materials and Methods.

$g' = 4.99$, 1350 G). Samples with essentially no NAS Fe^{3+} retained 0.85 Fe per SOD monomer.

The near absence of NAS Fe from our clean samples accounts for the significant difference between their EPR signal (Figure 1, curve 7) and the EPR spectrum of Fe^{3+}-sub-(Mn)SOD that has not been cleaned extensively (Figure 1, curve 4, and published examples). In contrast to previous reports, we find that the neutral pH EPR signal of clean Fe^{3+}-sub-(Mn)SOD is quite unlike that of Fe^{3+}-SOD at any pH. The optical spectrum of clean Fe^{3+}-sub-(Mn)SOD at low pH resembles those in the literature (9, 15), and appears in Figure 3. Fe^{3+}-sub-(Mn)SOD absorbs wavelengths up to 450 nm but lacks Fe^{3+}-SOD's clear absorption maximum at 350 nm (29). All optical characterizations described below were performed on Fe^{3+}-sub-(Mn)SOD containing Fe^{3+} only in the active site, and EPR spectra were collected at the end of titrations to assess the degree of Fe release during the titration. Less clean material was used in EPR characterizations, but only changes in features ascribed to the active site Fe^{3+} are described.

The Active Site of Reduced Fe^{2+}-sub-(Mn)SOD. The active site of (reduced) Fe^{2+}-sub-(Mn)SOD is compared with that of Fe^{2+}-SOD by ^{1}H NMR in Figure 2. Paramagnetism from the high-spin Fe^{2+} ion shifts the resonances of residues in
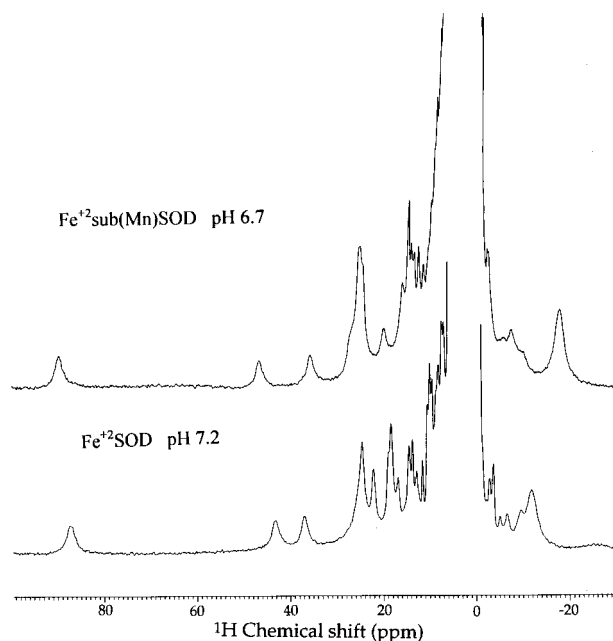
FIGURE 2: ^1H NMR spectra of reduced Fe^{2+}-sub-(Mn)SOD (top) and Fe^{2+}-SOD (bottom) obtained at 30 °C. The samples were at pHs 6.7 and 7.2, respectively, and contained indicator molecules and DSS as described under Materials and Methods.
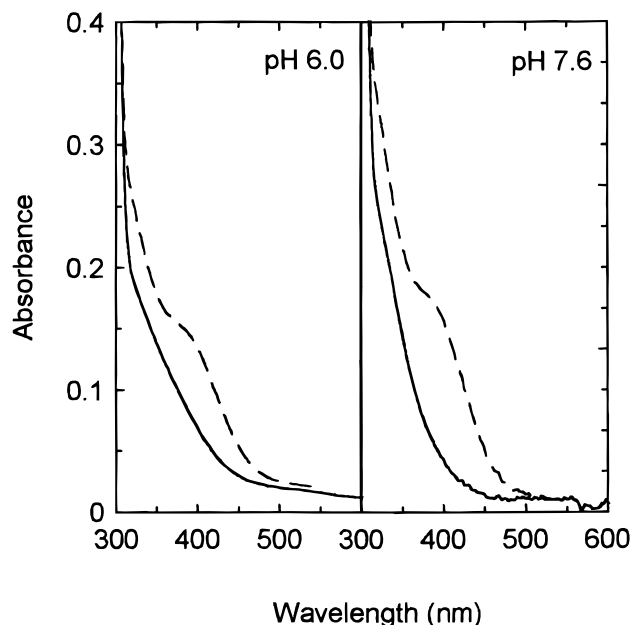

FIGURE 3: Effect of azide binding on the optical spectrum of oxidized Fe^{3+}-sub-(Mn)SOD. Left: optical spectra of Fe^{3+}-sub-(Mn)SOD at pH 6 in the absence (solid line) and presence of N_3^- (dashed line). The latter spectrum was obtained in the presence of saturating N_3^-, (= 1.5 mM). Right: optical spectra of Fe^{3+}-sub-(Mn)SOD at pH 7.6 in the absence (solid line) and presence of N_3^- (dashed line). The latter spectrum was obtained in the presence of saturating N_3^-, (= 4 mM). Spectra were obtained at 25 °C in a buffer composed of 100 mM KH_2PO_4/100 mM KBr, as described under Materials and Methods.

and near the active site out of the diamagnetic envelope. Although individual resonance positions are different in the two proteins, Fe^{2+}-sub-(Mn)SOD has a similar pattern of paramagnetically shifted resonances to Fe^{2+}-SOD, despite the extreme sensitivity of paramagnetic chemical shifts to differences in the electronic structure of the paramagnet and the conformation of the active site. Both spectra display

three strongly shifted resonances with one near 80 ppm and the other two near 40 ppm. All three protons exchange with solvent with the one resonating just above 40 ppm exchanging on a time scale of milliseconds and the other two exchanging more slowly in both cases. Thus, these three resonances in Fe^{2+}-sub-(Mn)SOD appear to represent the same ligand His δNH protons (*30*) as the analogous resonances in Fe^{2+}-SOD.

The NMR spectrum of Fe^{2+}-sub-(Mn)SOD is sensitive to pH, similar to that of Fe^{2+}-SOD. Consistent with their assignment to homologous protons, the three resonances between 35 and 80 ppm shift in the same directions in Fe^{2+}-sub-(Mn)SOD and Fe^{2+}-SOD as the pH is increased, and plots of the chemical shift vs pH, for several different resonances, all indicate a pK of 9.1 ± 0.1. This value is slightly higher than the pK of Fe^{2+}-SOD of 8.5 (*21*). In addition, the resonance at 46.8 ppm became completely saturated at high pH presumably due to saturation transfer from solvent, similar to the analogous resonance of Fe^{2+}-SOD which becomes 50% saturated. The greater accessibility to exchange of the ligand His δNH proton corresponding to the 46.8 ppm resonance of Fe^{2+}-sub-(Mn)SOD may be related to the lower stability of Fe^{2+}-sub-(Mn)SOD via a less rigid active site structure.

The Oxidized Fe^{3+}-sub-(Mn)SOD: Altered Substrate Analogue Binding and pKs. The ability of Fe^{3+}-sub-(Mn)SOD to bind N_3^- and F^- was used as a proxy for ability to bind the substrate, $O_2^{\bullet-}$. Upon binding N_3^-, a pronounced shoulder develops in the optical spectrum at ≈400 nm [Figure 3 and (*10, 15*)]. However, the spectrum is less intense at longer wavelengths (or less red-shifted) than the spectrum of N_3^--ligated Fe^{3+}-SOD (*29*). Titrations yielded an apparent dissociation constant at low pH of $K_D' = 90$ μM instead of Fe^{3+}-SOD's larger low pH K_D' of 2.1 mM (*12, 29*). Thus, we confirm that Fe^{3+}-sub-(Mn)SOD binds N_3^- at least 10 times more tightly than does Fe^{3+}-SOD.

Comparison of the EPR spectra of the N_3^- and F^- complexes of Fe^{3+}-sub-(Mn)SOD with that of unligated Fe^{3+}-sub-(Mn)SOD clearly shows that both of these anions coordinate to Fe^{3+}, as in Fe^{3+}-SOD (Figure 4). Our spectrum of F^--bound Fe^{3+}-sub-(Mn)SOD looks similar to the intermediate signal formed upon ligation of 1 equiv of F^- to Fe^{3+}-SOD, although F^--Fe^{3+}-SOD's EPR spectrum is a complicated superposition of three different signals because Fe^{3+}-SOD binds 2 equiv of F^- in succession (*29*). The signal we obtain from N_3^--Fe^{3+}-sub-(Mn)SOD is distinctly different from that of N_3^--Fe^{3+}-SOD (*29*) as also noted by (*15*).

pH Titrations. The changes in the optical spectrum of Fe^{3+}-sub-(Mn)SOD upon alkalinization parallel those previously reported [Figure 3 and (*9, 15*)] with apparent bleaching possibly due to a shift to shorter wavelengths. EPR confirms that Fe is not released upon addition of KOH up to at least pH 10. The change in absorbance at 370 nm as a function of pH reveals two pH transitions, with pKs equal to 6.7 ± 0.1 and 8.5 ± 0.3 (Figure 5). Assumption of a single pK yields a considerably poorer fit to the data, which clearly display the inflection near pH 8.5. Although a second, higher pK has not been claimed before, a similar pK has been invoked to fit activity vs pH data (*28*), and the effect we observe appears to be present in a published optical pH titration as well (*15*).
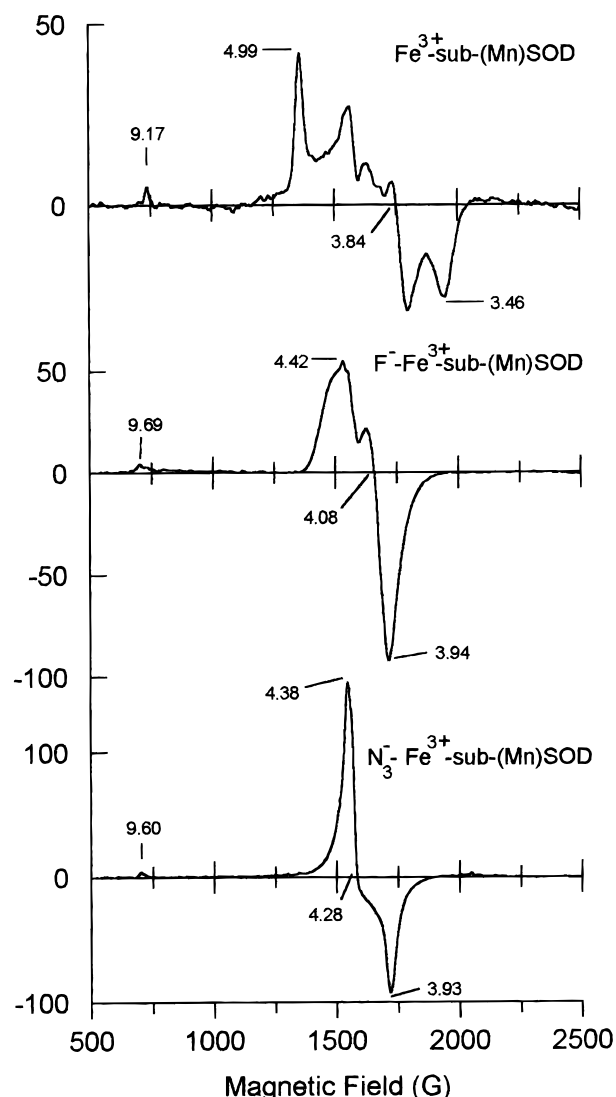
FIGURE 4: EPR spectra of free Fe^{3+}-sub-(Mn)SOD in 50% glycerol (top), F^--bound Fe^{3+}-sub-(Mn)SOD (middle), and N_3^--bound Fe^{3+}-sub-(Mn)SOD (bottom). Samples contained 0.1 mM Fe^{3+}-sub-(Mn)SOD in a buffer composed of 100 mM KH_2PO_4, pH 7.4, to which was added glycerol (final concentration 50% v/v), NaF (25 mM final concentration), or NaN_3 (2.5 mM final concentration). The Fe^{3+}-sub-(Mn)SOD preparation used contained a small but common quantity of NAS Fe evident in the top spectrum between 1500 and 1600 G ($g' = 4.3$). This species is still present, but less evident in the spectra of ligated Fe^{3+}-sub-(Mn)SOD because the active site Fe^{3+} is converted to a form whose signal overlaps with and obscures that of NAS Fe. Note the different vertical axes used for the three spectra. The g' values of prominent spectral features are indicated.

The pK of 6.7 appears to be associated with decreased affinity for N_3^-. Although individual azide titrations were well-behaved and conformed to a single binding event (Figure 6), the K_D' increased with increasing pH to 203 ± 5 μM at pH 6.75 and 9 ± 0.06 mM at pH 9.0. The pH dependence of the K_D' is consistent with an event mutually exclusive of N_3^- binding associated with a pK of 7, or requirement of a proton with p$K = 7 ± 0.1$ for N_3^- binding (Figure 7). The similarity between this pK and the optical pK of 6.7 suggests that the two correspond to the same event. Thus, our data agree with those on *S. marcescens* (*10*), that the pK affecting anion binding is considerably lower in Fe^{3+}-sub-(Mn)SOD than in Fe^{3+}-SOD. However, our value of
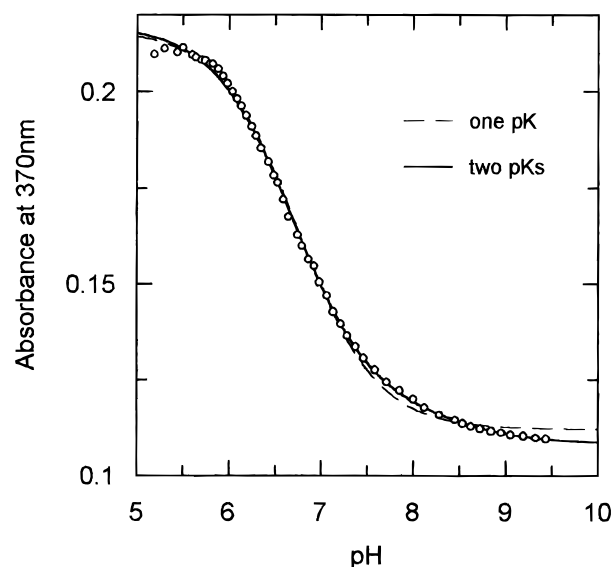

FIGURE 5: pH titration of Fe^{3+}-sub-(Mn)SOD based on the change in absorbance at 370 nm. The dashed curve represents a fit to the data of the Henderson−Hasselbalch equation for a single pK (yielding a pK of 6.7 ± 0.1), and the solid curve represents a fit to the data assuming two pKs (yielding pKs of 6.7 ± 0.1 and 8.5 ± 0.3). The same result is obtained using other wavelengths, the absorbance at 600 nm was subtracted from that at 370 nm to correct for base line fluctuations, and titrations were performed at 25 °C in a buffer composed of 100 mM KH_2PO_4/100 mM KBr, as described under Materials and Methods.
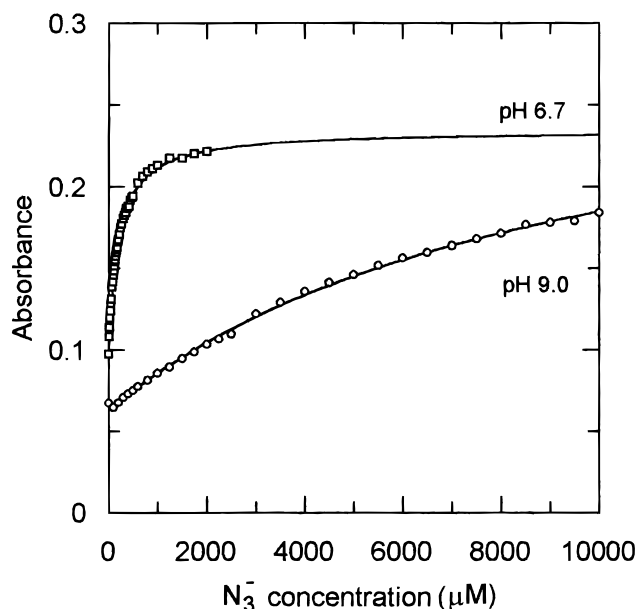

FIGURE 6: Titrations of Fe^{3+}-sub-(Mn)SOD with N_3^- based on the optical absorbance at 390 nm. Titrations were performed at 25 °C in a buffer composed of 100 mM KH_2PO_4/100 mM KBr, as described under Materials and Methods. Titrations obtained at pHs 6.75 (□) and 9.0 (○) are compared.

6.7−7 agrees better with the value of 6.4 for *E. coli* Fe^{3+}-sub-(Mn)SOD (*15*) than the value of 6.1 (9).

EPR spectroscopy probes the metal ion directly and thus provides a means of separating protein- and metal-derived contributions to changes in the optical spectrum. Elevation of the pH gives rise to a dramatic change in the EPR signal from relatively rhombic-looking[4] with g' values of 4.99, 3.84, and 3.46 at pH 7, to a very broad signal with $g' = 8.0 ± 0.3$ and 5.2 ± 0.1 (Figure 8). Although the high-pH sample
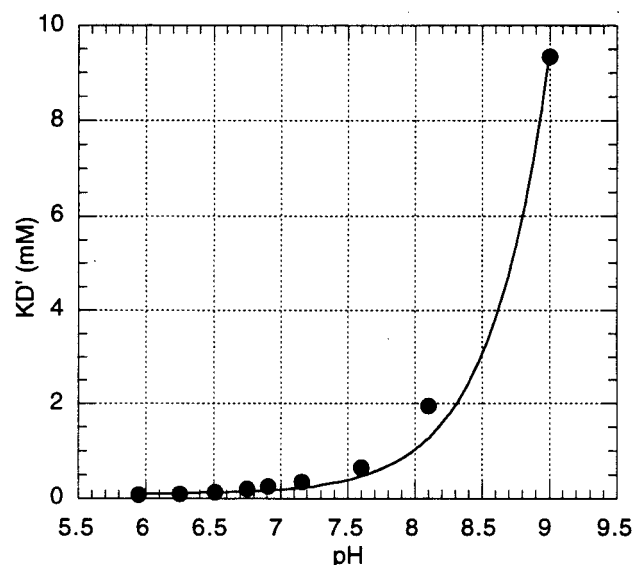
FIGURE 7: pH dependence of the apparent dissociation constant K_D' of Fe^{3+}-sub-(Mn)SOD for N_3^-. Samples of 0.1 mM Fe^{3+}-sub-(Mn)SOD in 100 mM KH_2PO_4/100 mM KBr were titrated as described under Materials and Methods. The solid line assumes mutually exclusive N_3^- binding and either OH^- binding or deprotonation, and yields a pK of 7.0 with a standard error of 0.02 assuming a low-pH asymptote of 90 μM, the K_D' at the lowest pH.

contained a small amount of NAS Fe^{3+}, the latter's signal did not appear to change with pH. Apart from the NAS Fe^{3+}, the spectrum of Fe^{3+}-sub-(Mn)SOD at high pH appears to be composed of a single signal that has ceased to change with further pH increases, and completely replaces the neutral pH signal. The pH dependence of the amplitude of the g' = 8.0 feature is described by a single pK of 8.5 $\pm$ 0.1 (Figure 9). The pH dependence of the features in the region of g' = 4−5 is more complicated, and indicative of at least one additional, lower pK. A feature at g' = 4.8 develops at lower pHs. However, we are not confident of having produced a sample containing a single low-pH species, even at the lowest pH accessible so far.

DISCUSSION

One of the long-standing mysteries of bioinorganic chemistry is why Fe-sub-(Mn)SOD appears inactive despite the strong structural and amino acid homologies between (Fe)SOD and (Mn)SOD proteins. Yamakura and colleagues have reported that the pK associated with substrate analogue binding and the optical spectrum is shifted to lower pH (*10*), Whittaker and Whittaker have shown that replacement of Tyr 34 with Phe ameliorates activity and shifts the low pK up closer to that of native Fe-SOD (*15*), and we have determined that Fe-sub-(Mn)SOD has a strongly depressed $E°$ and that it can mediate reduction, though not oxidation of $O_2^{•−}$ (*16*). Here, we seek to identify factors that could be related to Fe-sub-(Mn)SOD's low $E°$, as well as alternate reasons for Fe-sub-(Mn)SOD's specific inability to mediate oxidation of $O_2^{•−}$.

The current comparison of Fe-SOD and Fe-sub-(Mn)SOD reveals effects due to differences between the (Fe)SOD and (Mn)SOD proteins, as it represents a protein substitution
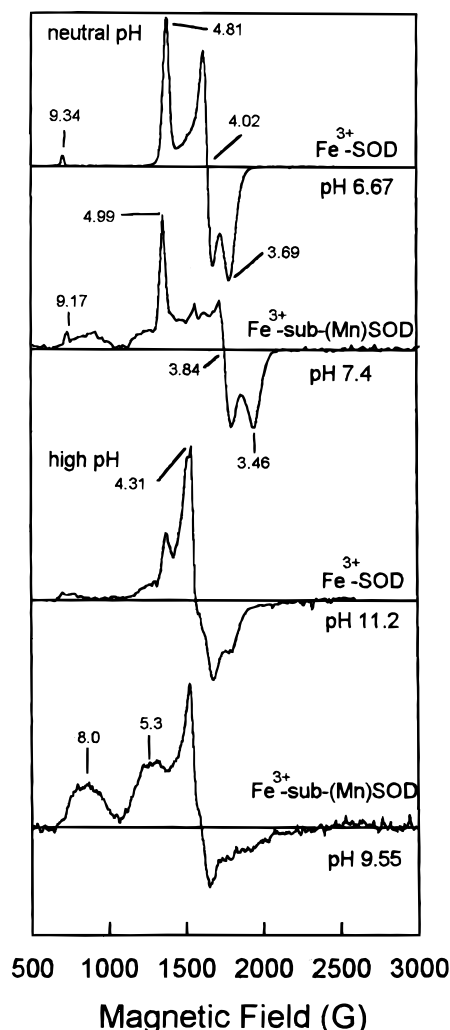

FIGURE 8: EPR signals of Fe^{3+}-SOD (top) and Fe^{3+}-sub-(Mn)-SOD (second) at neutral pH and Fe^{3+}-SOD (third) and Fe^{3+}-sub-(Mn)SOD (bottom) at high pH. The neutral pH spectrum of Fe-sub-(Mn)SOD contains a small contribution from the high pH signal. Samples contained 0.1 mM SOD in 100 mM KH_2PO_4, 100 mM KBr at the stated pHs. EPR conditions were as described under Materials and Methods. The g' values of prominent spectral features are indicated.

around the common Fe metal ion.[5] It also provides a base line for future characterizations of mutants of (Fe)SOD and (Mn)SOD with both Fe and Mn bound.

Discrimination between Fe Bound in the Active Site and Elsewhere. Fe can bind either outside the active site or in disrupted active sites, in Fe-SOD and Fe-sub-(Mn)SOD (*4, 25*). In Fe-SOD, a more rhombic EPR signal (g' = 4.3) was attributed to NAS Fe, whereas a less rhombic EPR signal (g' = 4.8−3.6) was attributed to native Fe^{3+}-SOD active sites as it was rapidly reduced by $O_2^{•−}$ and its intensity correlated with activity (*4*). An EPR signal analogous to the more rhombic signal (g' = 4.3) is present to varying degrees in most Fe-sub-(Mn)SOD preparations.

Comparison of samples with similar concentrations of active site Fe based on the amplitude of its EPR signal at g' = 4.99, but different amounts of total Fe, enabled us to

---

[4] *E/D* may not be sufficient to describe the EPR signals of Fe-SOD, as demonstrated beautifully by (*31*).

[5] It is not able to address the possibility that either protein's interactions with a given metal ion will produce properties that depend on the specific combination of protein and metal ion.
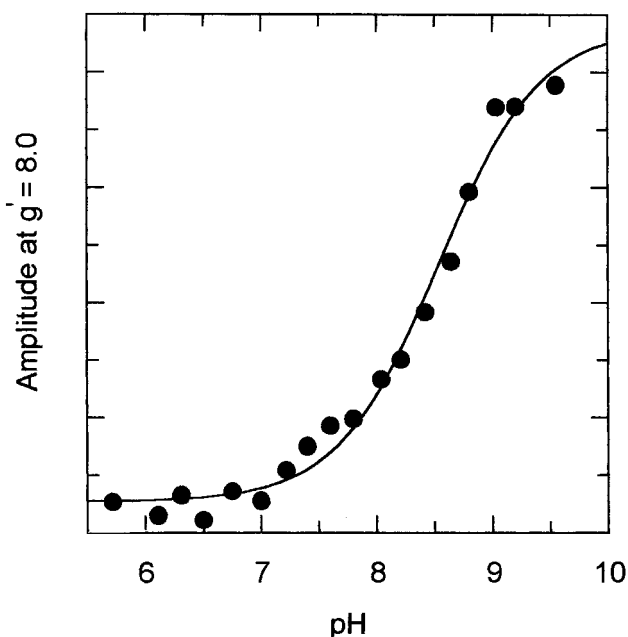
FIGURE 9: pH titration of Fe^{3+}-sub-(Mn)SOD based on the amplitude of the EPR feature at $g' = 8.0$. The titration and EPR conditions were as described under Materials and Methods. The signal amplitude at $g' = 8.0$ was corrected for sample concentration after base line correction.

correlate the amplitude of the $g' = 4.3$ signal with the (variable) amount of excess Fe, and indicated that Fe-sub-(Mn)SOD samples with typical EPR spectra (such as curve 4 in Figure 1) contain only ≈15% NAS Fe. Nonetheless, we find that the optical spectra of such samples are significantly more intense than those of samples without NAS Fe. Thus, even a little NAS Fe can make a substantial contribution to optically detected pH and anion binding titrations, and the pKs and K_Ds reported based on such studies do not reflect the active site alone unless NAS Fe has been scrupulously removed. The absence of NAS Fe from our preparations can explain the difference between our K_D and pK and those in the literature. Although our clean preparations yield a K_D for N_3^- of 90 μM at pH 6.0 and a pK of 6.7, preparations that had EPR signals similar to those in the literature displayed a K_D of 0.01 mM at pH 5.0 and a pK of 6.1, similar to the values previously reported (*15, 9*), respectively.

Reduced State of Fe^{2+}-sub-(Mn)SOD: Integrity of the Active Site and Competence for Proton Donation. Our characterizations yield clues, but not answers, as to why Fe-sub-(Mn)SOD is inactive. NMR spectroscopy indicates that the active sites of Fe^{2+}-SOD and Fe^{2+}-sub-(Mn)SOD are similar since they display three similar resonances ascribed to ligand His δNHs. The NMR resonances of residues in the active site are paramagnetically broadened and shifted depending on their proximity and through-bond connections with the Fe^{2+}. Paramagnetic contributions to chemical shift reflect the Fe^{2+} electronic state as well as the unpaired electron spin distribution among the valence orbitals, and the line widths of active site resonances are very sensitive to active site structure as they depend on the inverse sixth power of the protons' distances to Fe^{2+} (*32, 33*). Thus, the very similar chemical shifts and line widths of the ligand δNHs indicate that the electronic structure of Fe^{2+} and its interactions with its ligands are similar in the two proteins.

The reduced state is believed to supply at least one of the protons required in reaction 1b, probably from Tyr 34, whose pK of 8.5 has been identified in Fe^{2+}-SOD (*7*). The fact that the ligand His δNH resonances of Fe^{2+}-sub-(Mn)SOD respond to pH by shifting by comparable amounts in the same directions as analogous resonances of Fe^{2+}-SOD indicates that the same event is being monitored, i.e., the deprotonation of Tyr 34. This and the relatively small difference between the pK of 9.1 and the pK of Fe^{2+}-SOD are consistent with the fact that Fe-sub-(Mn)SOD remains active with respect to the reaction mediated by the reduced state, 1b (*16*). Finally, the similarity of the two pK values suggests that the (Mn)SOD protein produces an electrostatic potential that is only slightly more negative than that of (Fe)-SOD at the active site in the reduced state, with the difference being much too small to account for the different $E°$s.

Oxidized State of Fe^{3+}-sub-(Mn)SOD: Perturbation of the Active Site but Retention of Substrate Analogue Binding. The EPR signal of neutral pH Fe^{3+}-sub-(Mn)SOD is significantly different from that of Fe^{3+}-SOD, suggesting an altered ligand field in the oxidized state. However, additional experiments and spectral simulations possibly employing the general crystal field Hamiltonian including quartic terms and a distribution of E/D values (*31*) may be required for a more quantitative appreciation of the differences.

Since reaction 1b may proceed via an outer sphere mechanism (*34*) whereas reaction 1a is believed to be an inner sphere reaction (*29*), inability to bind substrates could explain Fe-sub-(Mn)SOD's inactivity specifically with respect to reaction 1a. The fact that the substrate analogue N_3^- binds more tightly to Fe^{3+}-sub-(Mn)SOD than Fe^{3+}-SOD argues that Fe^{3+}-sub-(Mn)SOD can also bind $O_2^{\bullet-}$. Furthermore, the EPR signal of F^--Fe^{3+}-sub-(Mn)SOD resembles the signal observed from singly F^--bound Fe^{3+}-SOD, suggesting that F^- binds to Fe^{3+} similarly in the two proteins. The EPR and optical signals of N_3^--Fe^{3+}-sub-(Mn)SOD are different from those of N_3^--Fe^{3+}-SOD (also see ref *15*). However, it does not appear that inability to form a precursor complex explains why Fe^{3+}-sub-(Mn)SOD fails to mediate reaction 1a.

Deprotonation and OH^- Binding Events in the Oxidized Active Site That Could Be Related to $E°$. In Fe-SOD, reduction is coupled to proton uptake (*12*). Thus, the overall $E°$ observed reflects not only the $E°$ of the metal ion itself but also the pKs of the group that accepts the proton, in the reduced and oxidized states. Assuming that the same happens in Fe-sub-(Mn)SOD, a change in the pK of the group that takes up a proton, in either oxidation state, would contribute to an altered $E°$. Moreover, any ionizable residue close enough to Fe to interact electrostatically with it, and any hydrogen bonding group that donates or accepts hydrogen bonds to the ligands, will also affect the $E°$. Thus, the pKs of residues in and around the active site are closely related to the Fe $E°$.

The Lower pK. Optical titrations of Fe^{3+}-sub-(Mn)SOD reveal two pKs, one with a large (absolute) effect on ϵ_{370} with p$K = 6.7 \pm 0.1$ and another with a 10-fold smaller effect with p$K = 8.5 \pm 0.3$. The lower pK appears to affect substrate analogue binding. However, it has subtle (if any) effects on the EPR spectrum, indicating that it does not correspond to OH^- binding to Fe^{3+}. Since the optical signal is ascribed to a LMCT, the change in ϵ_{370} might be due to

changes in the character of the ligand orbitals contributing to the ground state, with relatively minor changes in the metal orbitals. Thus, it appears to affect the protein's contribution to anion binding instead of the Fe's, and could perturb a protein site at which N_3^- binds prior to coordinating to Fe^{3+} [a "prebinding" site, by analogy with the two-step binding of N_3^- observed in Fe^{3+}-SOD (*11*)]. N_3^- (and F^-) binding could be disfavored by loss of a proton involved in hydrogen bonding to incoming anions, or by a decrease in the net positive charge of the active site and thus the latter's affinity for anions. The group responsible for the p*K* of 6.7 has not been identified, but it appears to interact with Tyr 34 since Y34F Fe-sub-(Mn)SOD retains the optical signature of the p*K* but at a modified p*K* value (*15*).

The alternate possibility of OH^- binding in the "prebinding" site raises the question of why N_3^- and F^- coordinate to Fe^{3+} but OH^- does not. Thus, one enigmatic difference between Fe^{3+}-SOD and Fe^{3+}-sub-(Mn)SOD is that whereas OH^-, N_3^-, and F^- all behave in qualitatively similar fashions in Fe^{3+}-SOD, binding in competition with one another and all affecting both the EPR and optical signals (*11, 12*), OH^- does not appear to coordinate to Fe^{3+} at the concentrations at which increasing pH inhibits N_3^- binding, and N_3^- does not appear to form a nativelike complex.

Finally, the observation that the EPR spectrum (at 65 K) and the optical spectrum (at 298 K) appear to depend on two different p*K*s is unlikely to be due to a temperature-dependent p*K*, as EPR spectra collected on a pH 7.3 sample contained comparable amounts of the low-pH signal at 65, 203, and 217 K. Since pH 7.3 is between the two p*K*s, the spectra should have contained less of the low-pH signal at the higher temperatures and more of the low pH signal at the lower temperatures if they were reflecting a single p*K* occurring at lower pH at higher temperature. Similarly, a pH 7.4 sample frozen as a glass in 50% glycerol produced a spectrum resembling those of samples frozen without glycerol (Figure 4, top curve, vs Figure 8).

The Higher pK. Although this is the first formal report of a p*K* of 8.5 in Fe^{3+}-sub-(Mn)SOD, evidence for such a p*K* can be seen in published optical data (*15*) and our EPR pH titration. Although our high-pH EPR spectrum is completely unlike that of Fe^{3+}-SOD, the difference between it and the high-pH spectra of Fe^{3+}-sub-(Mn)SOD in ref *10* may be largely due to the presence of more NAS Fe^{3+} in the latter. Moreover, there is a strong resemblance between our high-pH spectrum and the (extremely clean) spectrum in ref *15*.[6]

The dramatic effect of this p*K* on the EPR signal suggests that it corresponds to a change in the ligand sphere of Fe^{3+}, such as OH^- coordination, by analogy with Fe^{3+}-SOD. However, the high-pH EPR spectrum of Fe^{3+}-sub-(Mn)SOD does not resemble that of Fe^{3+}-SOD, indicating that the event has different effects on the active site in Fe^{3+}-sub-(Mn)SOD.

The apparently weaker effect on the optical signal is deceptive, since the optical signal is already strongly shifted or quenched by the lower p*K*. Similarly, OH^- might still act as a competitive inhibitor of substrate analogue binding, except that the latter is already too weak to be distinguished from nonspecific effects as a result of the lower p*K*. Thus, lowering of the p*K* of some other event to a value lower than the p*K* describing OH^- binding could result in many of the native consequences of OH^- binding being displayed "first" and more dramatically in connection with the other event.

CONCLUDING REMARKS

It is tempting to draw parallels between the pH dependencies of Fe^{3+}-sub-(Mn)SOD and native Fe^{3+}-SOD. However, the p*K* that affects anion binding in Fe^{3+}-sub-(Mn)SOD is 2 pH units lower than in Fe^{3+}-SOD and is not associated with a large change in the EPR spectrum. In Fe^{3+}-sub-(Mn)-SOD, an additional p*K* with a value similar to that of Fe^{3+}-SOD (8.5 vs 8.5–9) is associated with a dramatic change in the EPR signal, but the resulting signal is very different from that of OH^--Fe^{3+}-SOD. Thus, it is not clear which p*K*s correspond to the same events in the two different proteins, and thus which ones' values ought to be compared.

Nonetheless, it is very likely, considering the similar compositions of the two proteins' active sites, that the same events occur in Fe^{3+}-sub-(Mn)SOD as in Fe^{3+}-SOD. If so, our data indicate that their effects on the active site are different and that they may not occur in the same order. The presence, protonation states, and p*K*s of coordinated solvent can have important effects on $E°$, as can the ionization and hydrogen bonding states of other ligands and residues in the second sphere. Therefore, the altered p*K*s observed in Fe^{3+}-sub-(Mn)SOD could constitute a qualitative basis for its low $E°$, along with an altered ligand field as indicated by the nonnative EPR signals.

ACKNOWLEDGMENT

---

[6] The apparent difference between the pHs used in (*15*) and here to produce the high-pH EPR signal may be due to the instability of sample pHs upon freezing. We found that the pH could be up to 1.5 pH units different upon thawing a sample than when the sample was initially frozen. When only EPR samples whose pHs had changed less than 0.2 pH unit were considered, our high-pH titration of Fe^{3+}-SOD replicated the results of Fee (*11*) with respect to both the EPR signals and the p*K*. Thus, only EPR samples whose pH was stable within 0.2 pH unit were included in our titration of Fe^{3+}-sub-(Mn)SOD.

REFERENCES

1. Holm, R. H., Kennepohl, P., and Solomon, E. I. (1996) *Chem. Rev. 96*, 2239–2314.
2. Kiefer, L. L., Paterno, S. A., and Fierke, C. A. (1995) *J. Am. Chem. Soc. 117*, 6831–6837.
3. Goodin, D. B., and McRee, D. E. (1993) *Biochemistry 32*, 3313–3324.
4. Lavelle, F., McAdam, M. E., Fielden, E. M., Roberts, P. B., Puget, K., and Michelson, A. M. (1977) *Biochem. J. 161*, 3–11.
5. Lah, M. S., Dixon, M. M., Pattridge, K. A., Stallings, W. C., Fee, J. A., and Ludwig, M. L. (1995) *Biochemistry 34*, 1646–1660.
6. Stallings, W. C., Metzger, A. L., Pattridge, K. A., Fee, J. A., and Ludwig, M. L. (1991) *Free Radical Res. Commun. 12–13*, 259–268.
7. Sorkin, D. L., Duong, D. K., and Miller, A.-F. (1997) *Biochemistry 36*, 8202–8208.
8. Ose, D. E., and Fridovich, I. (1976) *J. Biol. Chem. 251*, 1217–1218.

9. Yamakura, F., Matsumoto, T., and Kobayashi, K. (1994) in *Frontiers of reactive oxygen species in biology and medicine*, (Asada, K., and Yoshikawa, T., Eds.) pp 115−118, Elsevier Science, Amsterdam.

10. Yamakura, F., Kobayashi, K., Ue, H., and Konno, M. (1995) *Eur. J. Biochem. 227*, 700−706.

11. Fee, J. A., McClune, G. J., Lees, A. C., Zidovetzki, R., and Pecht, I. (1981) *Isr. J. Chem. 21*, 54−58.

12. Bull, C., and Fee, J. A. (1985) *J. Am. Chem. Soc. 107*, 3295−3304.

13. Tierney, D. L., Fee, J. A., Ludwig, M. L., and Penner-Hahn, J. E. (1995) *Biochemistry 34*, 1661−1668.

14. Scherk, C., Schmidt, M., Nolting, H.-F., Meier, B., and Parak, F. (1996) *Eur. Biophys. J. 24*, 243−250.

15. Whittaker, M. M., and Whittaker, J. W. (1997) *Biochemistry 36*, 8923−8931.

16. Vance, C. K., and Miller, A.-F. (1998) *J. Am. Chem. Soc. 120-(3)*, 461−467.

17. Miller, A.-F., and Sorkin, D. L. (1997) *Comments Mol. Cell. Biophys. 9(1)*, 1−48.

18. Stein, J., Fackler, J. P., McClune, G. J., Fee, J. A., and Chan, L. T. (1979) *Inorg. Chem. 18(12)*, 3511−3519.

19. Barrette, J., W. C., Sawyer, D. T., Fee, J. A., and Asada, K. (1983) *Biochemistry 22*, 624−627.

20. Carlioz, A., and Touati, D. (1986) *EMBO J. 5*, 623−630.

21. Sorkin, D. L., and Miller, A.-F. (1997) *Biochemistry 36*(16), 4916−4924.

22. McCord, J. M., and Fridovich, I. (1969) *J. Biol. Chem. 244*, 6049−6055.

23. Beauchamp, C., and Fridovich, I. (1971) *Anal. Biochem. 44*, 276−287.

24. Beyer, W. F., Jr., and Fridovich, I. (1987) *Biochemistry 26*, 1251−1257.

25. Ose, D. E., and Fridovich, I. (1979) *Arch. Biochem. Biophys. 194*, 360−364.

26. Inubishi, T., and Becker, E. D. (1983) *J. Magn. Reson. 51*, 128−133.

27. Markley, J. L. (1975) *Acc. Chem. Res. 8*, 70−80.

28. Yamakura, F., Kobayashi, K., Tagawa, S., Morita, A., Imai, T., Ohmori, D., and Matsumoto, T. (1995) *Biochem. Mol. Biol. Int. 36*(2), 233−240.

29. Slykhouse, T. O., and Fee, J. A. (1976) *J. Biol. Chem. 251*, 5472−5477.

30. Ming, L.-J., Lynch, J. B., Holz, R. C., and Que, L., Jr. (1994) *Inorg. Chem. 33*, 83−87.

31. Iakovleva, O., Parak, F., Rimke, T., Meier, B., Hüttermann, J., and Kappl, R. (1995) *Eur. Biophys. J. 24*, 65−68.

32. LaMar, G. N., Horrocks, W. D., Jr., and Holm, R. H. (1973) in *NMR of Paramagnetic Molecules*, Academic Press, New York.

33. Bertini, L., and Luchinat, C. (1986) in *NMR of Paramagnetic Molecules in Biological Systems*, Benjamin/Cummings, New York.

34. Whittaker, J. W., and Solomon, E. I. (1988) *J. Am. Chem. Soc. 110*, 5329−5339.

35. Beyer, W. F., Jr., and Fridovich, I. (1991) *J. Biol. Chem. 266*, 303−308.

36. Carter, P. (1971) *Anal. Biochem. 40*, 450−458.